JOURNAL OF MATERIALS SCIENCE 16 (1981) 373–383

Non-equilibrium grain-boundary segregation in austenitic alloys

R. G. FAULKNER
Department of Materials Engineering and Design, Loughborough University of Technology, Loughborough, Leicestershire, UK

The theory of non-equilibrium grain-boundary segregation is discussed with particular reference to recent ideas and data relating to boron grain-boundary segregation in Type 316 austenitic steel. The kinetics of the non-equilibrium grain-boundary segregation process are considered in depth and a model is developed which, it is hoped, will more realistically describe the magnitude and extent of the process. Reasonable agreement is found between the predictions of the model and experimental evidence for non-equilibrium boron, aluminium and titanium segregation to grain boundaries in austenitic steels. The model predicts, generally, that elements with large misfits with the matrix atoms will segregate most. Larger grain sizes lead to greater grain-boundary segregation. Also, the two critical heat-treatment parameters in non-equilibrium segregation are the solution-treatment temperature and the cooling rate from the solution-treatment temperature. Predictions of the worst combinations of these parameters for maximum non-equilibrium segregation to grain boundaries in austenitic steels are presented.

1. Introduction

Non-equilibrium segregation and equilibrium segregation have similar origins. Equilibrium segregation occurs at interfaces such as grain boundaries and surfaces. It is caused by impurity atoms moving to interfaces and, as a result, reducing their free energy. Recently, the conditions necessary to cause equilibrium segregation have been reviewed by Seah and Hondros [1]. Their treatment concentrated on metals and showed that a simple relationship between the degree of segregation and temperature exists for binary systems. This relationship is of the form

$$\frac{c_b}{c_g} = A \exp\left(\frac{E}{kT}\right) , \qquad (1)$$

where c_b is the segregating atom concentration on the boundary to which segregation is occurring, c_g is the segregating atom concentration in the unsegregated regions, A is a constant, k is Boltzmann's constant and T is the absolute temperature. E is the free energy of segregation, that is, the reduction in energy of the segregating atom in the segregated site, e.g. a grain boundary. Usually atoms with large free energies of segregation have large differences in size and electronic structure compared to the matrix atoms [2]. Refinements in the calculation of E have recently been proposed for multi-element systems by Guttmann [3].

Although the magnitude of segregation at the interface is given by Equation 1, no account is taken of the variation of segregation with time. This is a significant omission because diffusion of the segregating species is an important aspect of the segregation mechanism. McLean [4] and Seah [5] have included an appraisal of the kinetics of equilibrium segregation, with the result that the effect of time and temperature on temper embrittlement of steel by phosphorus has now been successfully predicted on the basis of equilibrium segregation [5].

Equation 1 shows that equilibrium segregation is greater at lower temperatures and for higher free energies of segregation.

Non-equilibrium segregation theory was established by Aust *et al.* [6] and Anthony [7]. The mechanism of non-equilibrium segregation relies

0022–2461/81/020373–11$03.10/0

on the formation of sufficient quantities of vacancy–impurity complexes. When the material is quickly cooled through a large temperature range the equilibrium concentration of vacancies, and thus complexes, is reduced. This true equilibrium concentration cannot be realised during fast cooling conditions except at vacancy sinks. Such sinks are interfaces like grain boundaries and surfaces. Thus vacancy concentration gradients are formed in quickly-cooled materials and there is a net flow of vacancies towards the vacancy sinks. The vacancy–impurity complexes are also carried down these gradients and impurity atoms are thus deposited at the sink. Impurity segregation then accumulates near the relevant interface.

Another way of explaining the effect is to postulate a reverse Kirkendall effect. In this explanation, vacancies are expected to diffuse down the concentration gradient to the sink interface. Consequently a reverse flow of solvent and impurity atoms is established according to the Kirkendall model. Because of the strong interaction between the segregating impurities and vacancies, the solvent atoms are much less restricted and, hence, a net increase in the concentration of impurities near to the sink is created.

In contrast with equilibrium segregation, non-equilibrium segregation is dependent on the binding energy of the impurity atom to a vacancy, which is similar to that of E, the free energy of equilibrium segregation. It is also related to the temperature range over which the fast cooling occurs and to the cooling rate. Furthermore, non-equilibrium segregation becomes greater when cooling from high temperatures, i.e. temperatures above which diffusion becomes significant.

Non-equilibrium segregation to grain boundaries has been investigated by Aust and Westbrook [8] and more recently by Williams *et al.* [9] and Marwick and Harries [10]. This paper considers non-equilibrium grain-boundary segregation in austenitic alloys and extends the theoretical treatment of Williams *et al.* to consider the kinetics of the process in more detail. Some experimental results on non-equilibrium segregation are presented which help to support the extended theory. The implications of the theory for heat-treatment procedures used in the heavy engineering metals industries are considered.

2. Quantification of non-equilibrium segregation

The technique used in this paper to quantify the process of non-equilibrium segregation to grain boundaries can be illustrated by Fig. 1. The *magnitude* of the effect is given by the ratio c_b/c_g. The *extent* of the effect is given by the distance away from the grain boundary, x, at which the concentration of impurity is reduced to minimal levels. The purpose of this paper is to quantify the variation in the shape of the curve with time, temperature and grain size. These parameters can be easily related to the practically important heat treatment parameters for austenitic alloys: the solution-treatment temperature and the cooling rate from the solution-treatment temperature.

2.1. Magnitude of non-equilibrium segregation

The magnitude of non-equilibrium segregation is determined assuming that only diffusion of complexes occurs. It simply indicates the change in concentration brought about at the vacancy sink during cooling from temperature T_i to $T_{0.5T_m}$, where T_i is the solution-treatment temperature and $T_{0.5T_m}$ is half of the melting temperature, T_m, of the austenitic steel matrix. This temperature is chosen because it is assumed that very little diffusion will occur below $T_{0.5T_m}$. The magnitude of the segregation can then be calculated assuming values of the thermodynamic free energies of vacancy impurity binding, E_b and of vacancy formation, E_f. The concentration of complexes, c_c, at temperature T is given by [9]

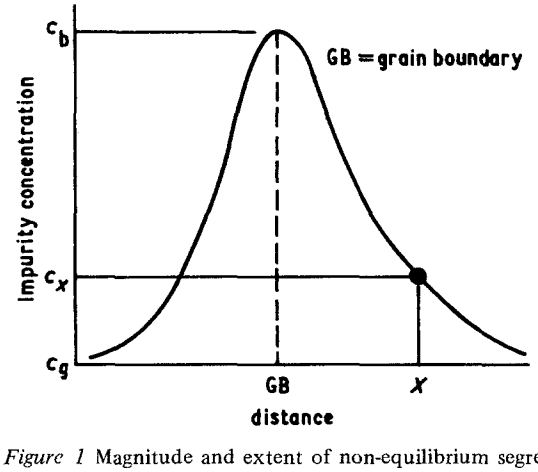

Figure 1 Magnitude and extent of non-equilibrium segregation.

$$c_c = k_c c_v c_I \exp\left(\frac{E_b}{kT}\right), \quad (2)$$

where c_v is the concentration of vacancies, c_I is the concentration of impurities, k_c is a geometrical constant and k is Boltzmann's constant. Now,

$$c_v = k_v \exp\left(\frac{-E_f}{kT}\right), \quad (3)$$

where k_v is a geometrical constant. Combining Equation 2 and Equation 3 gives

$$c_c = k_c k_v c_I \exp\left(\frac{E_b - E_f}{kT}\right). \quad (4)$$

It is now assumed that the material is cooled from T_i to $T_{0.5T_m}$ in a time sufficiently short that the isolated impurity atoms cannot move. At the sink the ratio c_c/c_I will decrease whereas this ratio will remain roughly constant in the grain centres where no vacancy sinks exist. The complexes will diffuse down the concentration gradients between the grain centres and grain boundaries in an effort to keep the concentration of complexes equal at all points. Therefore, an excess of impurities will be established at the grain boundaries. If it is assumed that, during the quench, an equilibrium is instantaneously established, appropriate to $T_{0.5T_m}$ on the grain boundary and appropriate to T_i at the grain centre, this excess can be represented as the inverse of the ratio of c_c/c_I predicted from Equation 4 for the sink, that is at $0.5T_m$. The magnitude of segregation is then indicated by the ratio of the excess impurity concentration at the sink, i.e. at $0.5T_m$, to the excess impurity concentration at the grain centres, i.e. at T_i. This is given by

$$\frac{(c_I/c_c)_{0.5T_m}}{(c_I/c_c)_{T_i}} = \exp\left[\frac{(E_b - E_f)}{kT_i} - \frac{(E_b - E_f)}{kT_{0.5T_m}}\right]. \quad (5)$$

This equation only relates to the ratio of impurity–complex concentrations. In this form it predicts that segregation will increase as E_b decreases, which is clearly not correct. Hence, a term must be included which indicates the absolute concentrations of complexes. This concentration must be related to the vacancy–impurity binding energy, E_b. E_b will rarely exceed E_f and, therefore, an approximate indication of complex concentration will be given by $f(E_b)$ where

$$f(E_b) = \frac{E_b}{E_f} \quad (6)$$

Multiplying the right-hand-side of the Equation 5 by Equation 6 gives the final equation describing the magnitude of non-equilibrium segregation, c_b/c_g:

$$\frac{c_b}{c_g} = \exp\left(\frac{(E_b - E_f)}{kT_i} - \frac{(E_b - E_f)}{kT_{0.5T_m}}\right)\frac{E_b}{E_f}. \quad (7)$$

Values of E_f are well-tabulated. In this work values of E_b were either taken from tabulated values or were calculated using elasticity theory. Following the ideas of Cottrell [11], the following formula approximately describes the binding energy of a vacancy with a foreign atom which has a misfit, ϵ, with the matrix lattice:

$$E_b = 8\pi\mu r_0^3 \epsilon^2, \quad (8)$$

where μ is the shear modulus of the matrix, r_0 is the matrix atom radius and

$$\epsilon = \pm\left(\frac{r_I - r_0}{r_0}\right) \quad (9)$$

where r_I is the impurity atom radius. Electronic and valence differences between the matrix and impurity atoms are neglected in this treatment. The effect of E_b on the magnitude of non-equilibrium segregation, calculated from Equation 7 for different cooling ranges between T_i and $T_{0.5T_m}$, is shown in Fig. 2.

2.2. Extent of non-equilibrium segregation

All treatments of the kinetics aspects of non-equilibrium segregation relate the non-equilibrium segregation process to the diffusion constant at one single temperature, taken for convenience as the solution-treatment temperature, T_i. This means that, on cooling from T_i to $0.5T_m$, an effective time at temperature T_i can be calculated for any cooling rate, θ, or heat-treatment cycle. An effective time, t_θ, as a function of cooling rate, θ, is given by [12]

$$t_\theta = \frac{RkT_i^2}{\theta E_A}, \quad (10)$$

where k is Boltzmann's constant, R is a constant and E_A is the average activation energy for diffusion of complexes and impurities in the matrix.

If an isothermal step occurs in the heat-

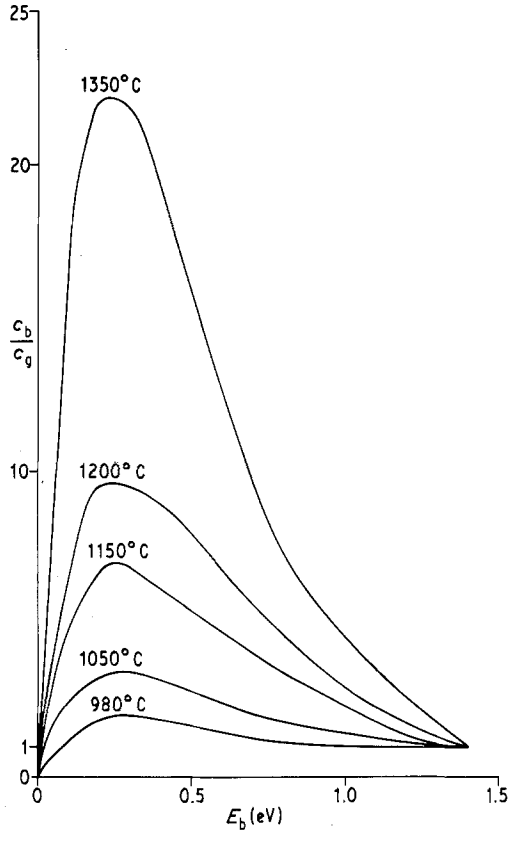

Figure 2 Effect of vacancy–impurity binding energy, E_b, on the non-equilibrium segregation magnitude, c_b/c_g, on cooling to 750° C from different solution-treatment temperatures.

treatment at a temperature T_A for a time, t_A, then the effective time at temperature T_i is calculated from

$$t_\theta = t_A \exp \frac{-E_A}{kT_iT_A}(T_i - T_A) \quad .. \quad (11)$$

Cooling and isothermal steps give values of t_θ which are additive. Thus, a final effective time, t_θ, for the heat-treatment at T_i is established.

During non-equilibrium segregation two distinct processes are occurring. These are segregation and de-segregation.

Firstly, impurities are drawn from the grains to the boundaries by motion of the complexes. The ratio of concentration of impurities, c_b, resulting on the boundaries relative to the matrix concentration, c_g, can never exceed that predicted by Equation 7. Thus, any accumulation of impurities must occur near to the grain boundary in a zone which extends outwards to an extent proportional to the amount of segregation taking place. An indication of the imagined concentration

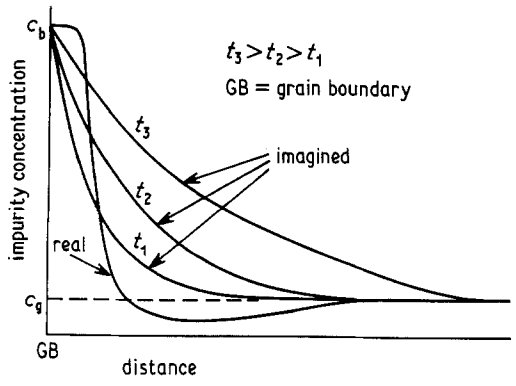

Figure 3 The segregation process.

profiles, quantified for different times, is shown in Fig. 3. This shows that, although the concentration of impurities remains constant on the boundary, at the equilibrium level, provision is made for an increasing concentration of impurities in the boundary region with increasing time. Of course, impurity removal from the grain centre will cause a depleted region for impurities outside the segregated zone and therefore, the real situation will be slightly different, as is also shown in Fig. 3. The model used here assumes the imagined set of curves because they can easily be quantified by applying the solution to Fick's Second Law for semi-infinite solids

$$\frac{c_x - c_g}{c_b - c_g} = erfc \frac{x}{2(D_v t_\theta)^{1/2}}, \quad (12)$$

where D_v is the complex diffusion coefficient and c_x is the concentration of impurity at a distance x from the grain boundary. Data on D_v are sparse and it is assumed here that D_v is given by the product of the frequency factor for vacancy diffusion and the exponential term containing the activation energy for diffusion of the impurity atom in the matrix. The *extent of segregation* when this process is occurring can be given approximately as

$$x_v = (D_v t_\theta)^{1/2}. \quad (13)$$

Secondly, when t_θ exceeds a critical time, t_c, the dominant effect is back diffusion, or de-segregation, of the impurity down the concentration gradient, towards the centre of the grain. The rate-determining step in this process is the impurity diffusion coefficient, D_I. The critical time after which de-segregation begins, t_c, is governed by the relative diffusion rates of the complexes towards the grain boundary and the

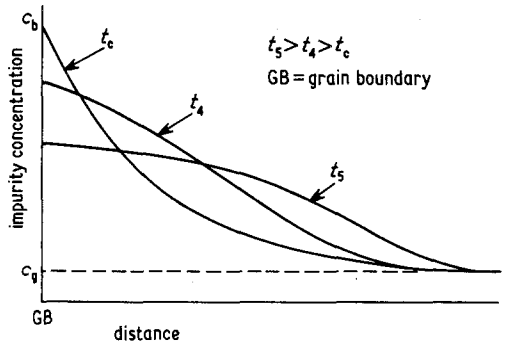

Figure 4 The de-segregation process.

diffusion rates of impurities away from the grain boundary and is given by

$$t_c = \frac{\delta d^2 \ln (D_v/D_I)}{4(D_v - D_I)}, \quad (14)$$

where δ is a numerical factor and d is the grain size. The derivation of this equation is given in Appendix 1.

During de-segregation the imagined composition profiles are as shown in Fig. 4. The situation can be described by the thin-film solution to the diffusion equation. Thus the concentration of impurity, c_x, at a distance, x, from the grain boundaries after time, t_θ (where $t_\theta > t_c$) is given by

$$\frac{c_x - c_g}{c_b - c_g} = \left(\frac{D_v t_c}{D_I t_\theta}\right)^{1/2} \exp\left(\frac{-x^2}{4D_I t_\theta}\right). \quad (15)$$

The derivation of this equation for the appropriate boundary conditions is given in Appendix 2. The impurity concentration on the grain boundary decreases during the de-segregation process. Appendix 2 also shows that the reduced grain boundary concentration, c_{x0}, is given by

$$\frac{c_{x0} - c_g}{c_b - c_g} = \left(\frac{D_v t_c}{D_I t_\theta}\right)^{1/2}. \quad (16)$$

The *extent of de-segregation* when this process is occurring can be given approximately as

$$x_I = (D_I t_\theta)^{1/2} \quad (17)$$

3. Results

Three cases of observed grain-boundary segregation believed to have occurred by a non-equilibrium segregation mechanism have been considered. These are:

(a) boron segregation in AISI Type 316 Steel [9];
(b) titanium segregation in 12R72 Steel [13];
(c) aluminium segregation in Inconel 600 [14].

In all three cases the matrix alloy is austenitic and the detailed compositions for the three alloys are given in Table I. The data used to theoretically calculate the non-equilibrium segregation for these three systems are given in Table II. The vacancy–impurity binding energy, E_b, was taken from the results of Williams *et al.* [9] for boron in Type 316 Steel. E_b for the titanium and aluminium cases were calculated from Equation 8. The concentration of impurities in the grain centres, c_g, was taken as the analysed concentration for the segregating atom, taken from Table I, converted to atomic per cent.

Non-equilibrium segregation is considered for various solution-treatment temperatures and cooling rates in the boron case. A combined 50° C sec^{-1} cooling rate and isothermal treatment for 10 hours at 850° C was undertaken for the titanium case. Finally, a simple cooling process at 2° C sec^{-1} was adopted for the aluminium case. Table III shows the calculated values of t_c and t_θ together with the resulting theoretical predictions of the non-equilibrium segregation magnitude, c_b or c_{x0}, and extent, x_v or x_I, for these heat treatments. These are listed in order of increasing magnitude for the boron case. The concentration of impurity atoms on the grain boundary, c_b, was found from Fig. 2 by taking the ratio c_b/c_g for the particular vacancy–impurity binding energy and cooling range considered. Knowing c_g, c_b could then be calculated. The values of c_{x0}, x_v and x_I were calculated from Equations 13, 16 and 17, respectively. A value of $R = 0.01$ is used to calculate t_θ and t_c is calculated using a value of δ of 5×10^{-2}.

TABLE I Alloy compositions

Alloy	Composition (wt %)											
	C	Si	Mn	Ni	Cr	Mo	Co	N	B	Ti	Fe	Al
Type 316	0.039	0.32	1.54	11.4	17.3	2.5	0.037	0.023	0.0018	–	balance	–
12R72*	0.11	0.44	2.0	14.8	15.2	1.4	–	–	–	0.52	balance	–
INCONEL 600	0.04	0.11	0.38	74.4	15.7	0.08	0.05	0.006	–	0.24	8.6	0.28

*Trade mark of Sandvik AB

TABLE II Data used in theoretical calculations

Parameter	Segregation case		
	B in Type 316 Steel	Ti in 12R72 Steel	Al in Inconel 600
$D_I(m^2\ sec^{-1})$	$2 \times 10^{-7} \exp\left(\frac{-0.91}{kT}\right)$ [17]	$1.5 \times 10^{-5} \exp\left(\frac{-2.6}{kT}\right)$ [18]	$1.87 \times 10^{-4} \exp\left(\frac{-2.8}{kT}\right)$ [19]
$D_v(m^2\ sec^{-1})$	$5 \times 10^{-5} \exp\left(\frac{-0.91}{kT}\right)$ [20]	$5 \times 10^{-5} \exp\left(\frac{-2.6}{kT}\right)$ [20]	$3.36 \times 10^{-4} \exp\left(\frac{-2.8}{kT}\right)$ [21]
E_f(eV)	1.4 [9]	1.4 [9]	1.4 [9]
E_A(eV)	0.91	2.6	2.8
c_g(at%)	0.009	0.6	0.61
$T_{0.5T_m}$(° C)	750	750	750
$\mu(N\ m^{-2})$		5×10^{10}	5×10^{10}
ϵ		0.16	0.14
r_0(m)		1.25×10^{-10}	1.25×10^{-10}
r_I(m)		1.45×10^{-10}	1.43×10^{-10}
E_b(eV)	0.5 [9]	0.43	0.37

Table III also shows the experimentally-measured grain-boundary segregation parameters for the various cases and heat treatments considered. The grain sizes, d, were measured by the assessment of optical micrographs. The observed non-equilibrium segregation magnitude, c_{obs}, and observed extent, x_{obs}, were measured by the assessment of autoradiographs for the boron segregation [9]. The autoradiographic technique has a spatial resolution of about 3.0 μm and there is no quantitative indication of the segregation magnitude given by this method. Thus the magnitude has been recorded in relative order of increasing magnitude in Table III. Where no segregation has been observed, the extent was put at less than 1.5 μm. The titanium and aluminium segregation was measured experimentally by the newly developed Scanning Transmission Electron Microscope with Microanalysis (STEMMA) technique. Quantitative estimates of the non-equilibrium segregation magnitude and extent with a spatial resolution of 500 to 1000 Å [15] are possible with this method.

A graphical approach can also describe the segregation accumulation. From the required parameters in Tables II and III composition profiles can be calculated, by computer, as a function of cooling rate and T_i. The computer can then compile the various degrees of segregation for various conditions and display these results on a three-dimensional graph, as shown in Fig. 5. The vertical axis in Fig. 5, F, quantifies, in a relative manner, the area contained under the composition against distance curve in a zone of width 1000 Å located at the grain boundary. In Fig. 5, the segregation in such regions for the

TABLE III Experimental and theoretical results

System	T_i (° C)	θ (° C sec^{-1})	d (μm)	c_g (at%)	t_θ (for $R = 0.01$) ($\times 10^{-3}$ sec)	t_c (for $\delta = 5 \times 10^{-2}$) ($\times 10^{-3}$ sec)	Magnitude (at%)		Extent (μm)	
							$c_b(t_\theta < t_c)$ $c_{x_0}(t_\theta > t_c)$	c_{obs}	$x_v(t_\theta < t_c)$ $x_I(t_\theta > t_c)$	x_{obs}
Boron in	1350	500	60	0.009	5.0	3.3	0.56	N.O.	1.2	< 1.5
Type 316	1200	500	45	0.009	4.1	3.6	0.34	N.O.	0.78	< 1.5
stainless	1050	500	30	0.009	3.6	3.6	0.19	N.O.	0.52	< 1.5
steel	1350	50	60	0.009	50	3.3	0.17	High	3.8	2.5
	1200	50	45	0.009	41	3.6	0.10	Medium	2.5	2.0
	1050	50	30	0.009	36	3.6	0.05	Low	1.6	2.0
Titanium in 12R72 steel	1150	(50 + Age)	35	0.6	123	940	3.84	7.70	3.8	0.2
Aluminium in Inconel 600	980	2	27	0.61	0.24	89000	1.28	2.5	0.012	0.6

N.O. = Not Observed

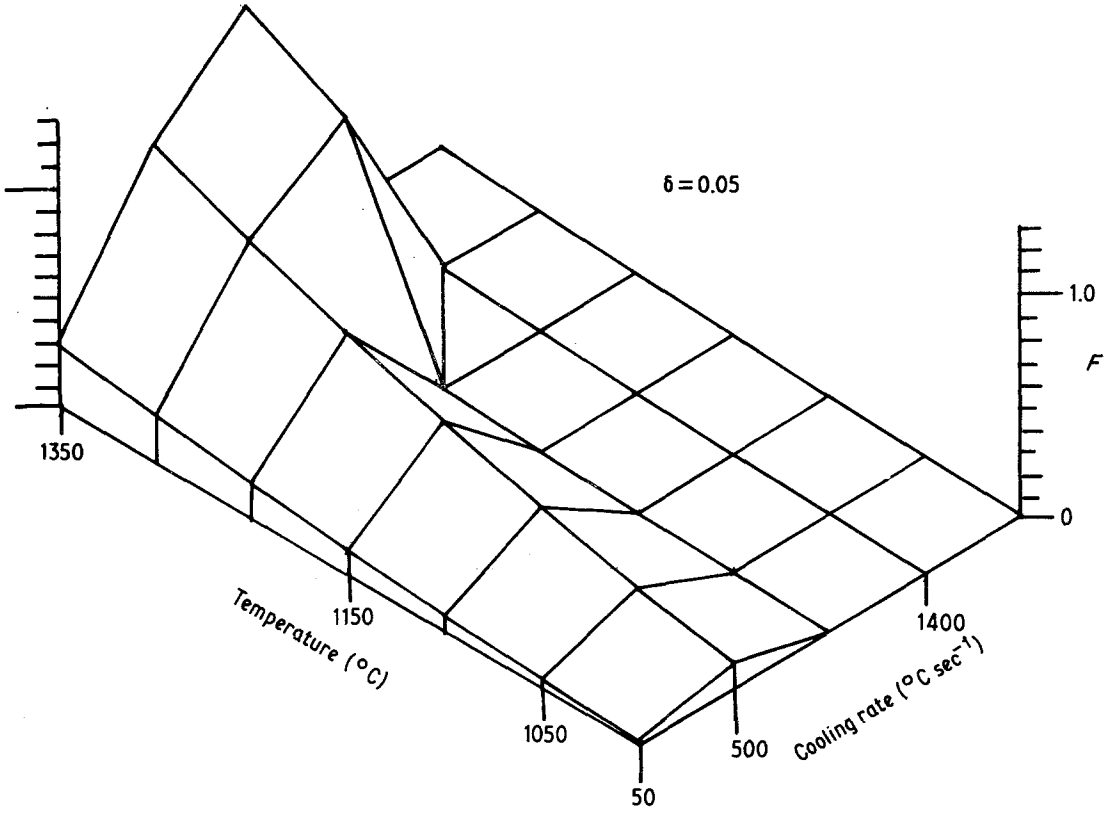

Figure 5 Effect of cooling rate, θ, and solution-treatment temperature, T_i, on amount of segregation within a distance of 1000 Å of the grain boundaries, F, for boron in Type 316 steel ($\delta = 0.05$).

case of boron in Type 316 Steel is shown. Similar graphs, with varying δ values are shown in Figs 6 and 7.

4. Discussion

Table III shows that reasonable agreement between the observed and the predicted non-equilibrium grain-boundary segregation is attained for the impurities in the austenitic matrices discussed in this work.

The extent of segregation predicted for boron is slightly over-estimated for the high solution-treatment temperatures and 50° C sec^{-1} cooling rates. The apparent disappearance of any segregation in the material cooled at a rate of 500° C sec^{-1} is clearly caused by the extent of segregation being too narrow to be resolved by the auto-radiographic method. It is worth commenting on the choice of δ and R so that $t_\theta > t_c$. If R and δ had been chosen so that $t_\theta < t_c$, then an extent of segregation of 38.5 μm would have been predicted for the alloy cooled at a rate of 500° C sec^{-1} and solution-treated at 1350° C. In the case of the titanium alloy the extent of segregation is slightly over-estimated, but the opposite is true for the aluminium alloy. The predicted extent of segregation is never more than a factor of 20 different from that observed except in the case of aluminium for which the difference is a factor of 40.

The segregation magnitudes for the boron case are difficult to compare because the auto-radiographic method gives no absolute indication of concentration. However, the experimentally-determined magnitude of segregation decreases with decreasing solution-treatment temperature and this agrees with the theoretical predictions. The aluminium and titanium cases both predict a slightly lower magnitude compared with that actually observed, but in neither case do the theoretical and experimental results differ by more than a factor of two. It must be mentioned here that the experimental STEMMA results are only reliable to within ± 10% as a result of absorption and fluorescence of the X-ray signals used to give quantitative results. At present it is impossible to give accurate quantitative information using the technique.

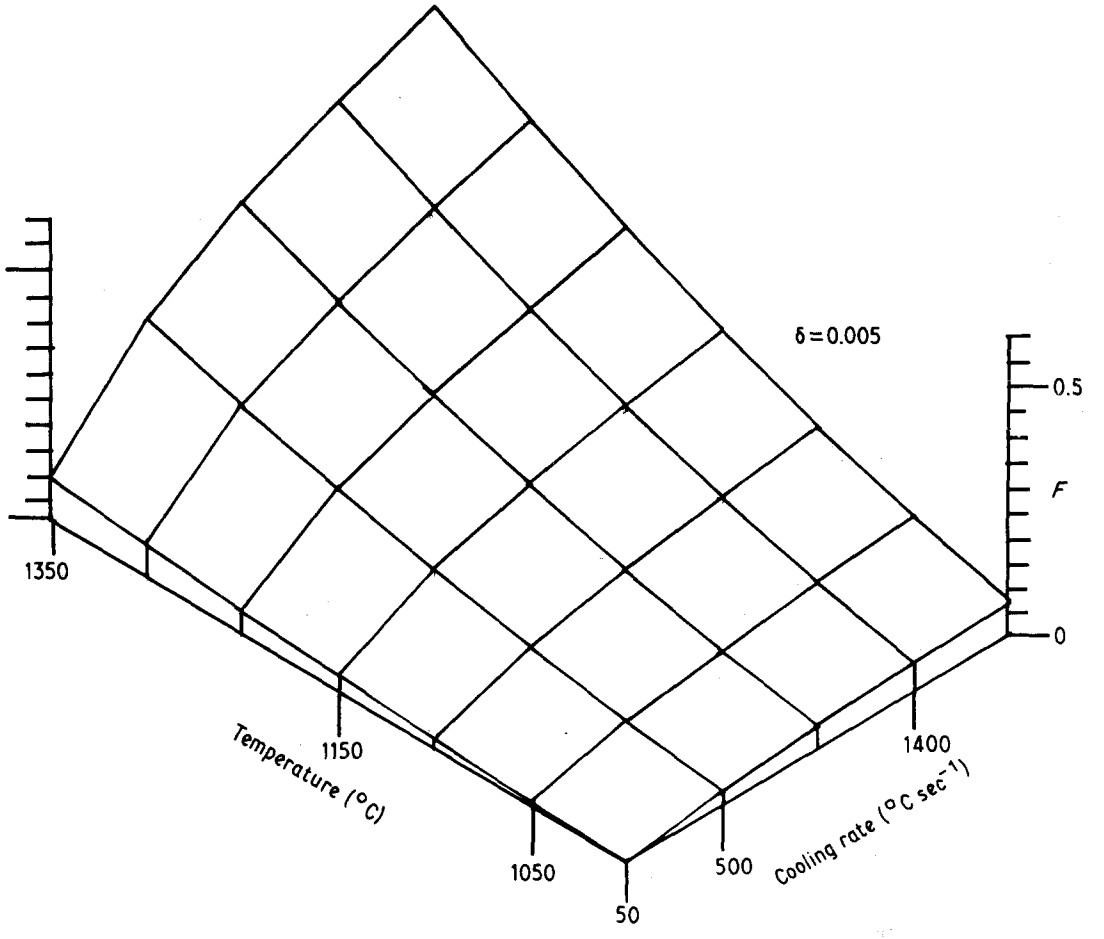

Figure 6 Effect of cooling rate, θ, and solution-treatment temperature, T_i, on amount of segregation within a distance of 1000 Å of the grain boundaries, F, for boron in Type 316 steel ($\delta = 0.005$).

In the titanium case there may be some contribution to the measured titanium concentrations from small, unresolvable titanium carbide particles on the grain boundary [13]. This would tend to artificially raise the measured concentration. In addition, recently published data on growth rates of titanium carbide particles on grain boundaries in a similar steel [16] suggest that there is an enhanced supply of titanium to the grain boundaries, suggesting that a titanium segregation of up to about five times the matrix level is occurring. This would imply a 3% titanium level at the grain boundaries in this alloy and this provides further experimental support for the theoretically predicted value of 3.84%.

The overall amounts of segregation measured from the areas under the composition profiles for zones within 1000 Å of the boundary, F, for the case of boron, are shown in Fig. 5. This confirms that segregation increases close to the boundary with increasing T_i and at cooling rates such that $t_\theta \simeq t_c$. The parameter F indicates that there should be more segregation for the material cooled at a rate of 500° C sec^{-1} than for the material cooled at a rate of 50° C sec^{-1}. However, it should be remembered that F only applies to the region very close to the grain boundary: the composition profile is more spread out for the 50° C sec^{-1} cooling rate. Thus, in this case, segregation is more easily observable with the autoradiographic technique used than for the material cooled at 500° C sec^{-1}.

The graphical approach can also be used to help select appropriate ratios of δ/R. Figs 6 and 7 show how the maximum segregation is shifted to much higher temperatures and lower cooling rates than that observed by increasing δ. Alternatively, the maximum segregation is located at faster cooling rates than those observed by reducing δ.

Discussion of the effect of R and δ on the

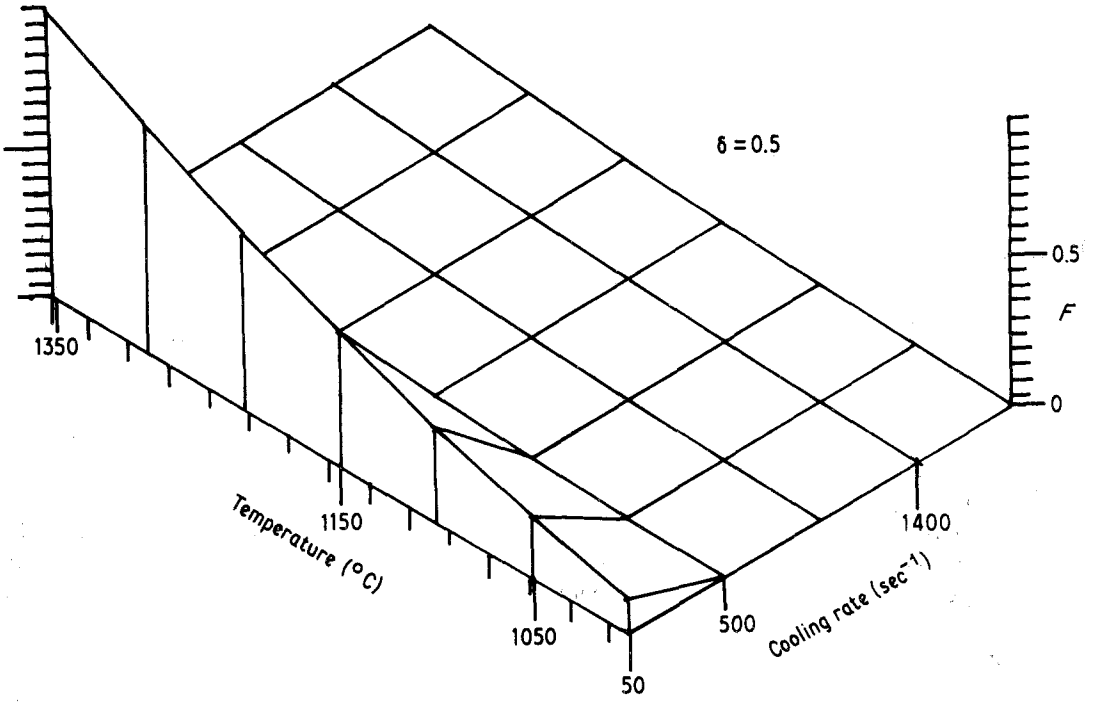

Figure 7 Effect of cooling rate, θ, and solution-treatment temperature, T_i, on amount of segregation within a distance of 1000 Å of the grain boundaries, F, for boron in Type 316 steel ($\delta = 0.5$).

theoretical results can be taken further. R, the numerical constant relating quench rate, θ, to a particular time of quench, t, at a given starting temperature, T_i, can be defined as follows [9]

$$R = 1 - \frac{\theta t}{T_i}. \qquad (18)$$

If the quench is from T_i to ambient temperature then R will be quite small and a value of 0.01 seems not unrealistic.

Williams *et al.* [9] have already used this effective time concept for the quench (Equation 10) and equated it to the time necessary to even out complex concentration differences between the grain centres and boundaries (Equation A5). The expression defining this homogenizing time involves a numerical constant describing the effectiveness of the diffusion process. This constant is the equivalent of approximately $\delta/4$ in this work. The approach of Williams *et al.* uses the ratio of $\delta/4R$ as a parameter, Λ_0, to indicate whether or not segregation will occur. The value chosen by Williams *et al.* was 0.6 ± 0.2. The values chosen in this work of $R = 0.01$ and $\delta = 5 \times 10^{-2}$ give a value of Λ_0 as 1.25. Thus the results quoted in this work, which give reasonable agreement between experiment and theory for a wider range of systems than were considered in the paper by Williams *et al.* [9], appear to substantiate the value of Λ_0 set by Williams *et al.* and to justify the use here of a value of δ of 5×10^{-2}.

Justification for the choice of the constants to describe the diffusion of vacancy–impurity complexes arises from consideration of the basic model. The model assumes that no non-equilibrium grain-boundary segregation will occur unless the complexes move faster than the impurity atoms. This will always be the case if the complexes move under the influence of the frequency factor associated with vacancies diffusing through the matrix and the activation energy associated with the diffusion of the impurities through the matrix. Since diffusion of complexes must take place by a combination of processes connected with vacancy and impurity diffusion, the above assumption seems reasonable.

The principle improvements offered by the model proposed in this paper over that of Williams *et al.* is that:

(a) de-segregation is considered in the kinetics appraisal;

(b) the extent or width of the segregated zone is quantified.

Thus, in certain circumstances, such as for boron

in AISI Type 316 steel, solution-treated at 1350° C and cooled at 500° C sec^{-1}, no segregation is predicted by the model of Williams *et al.* Considering the model proposed in this work, this is clearly not true: under those conditions there is segregation, but only over a narrow zone width. Hence, even segregated regions of widths more typical of equilibrium segregation (< 100 Å) can be predicted by this model. This fact has implications for heat-treatment engineers because embrittling effects are known to occur when precisely this kind of segregation occurs. Thus, the data contained in Figs 5, 6 and 7 are likely to contain the information most useful in practice.

The simplest guide to overcoming the grain boundary non-equilibrium segregation problem centres on cooling from such a solution-treatment temperature and at such a rate that $t_\theta \gg t_c$ for the system being considered. A high solution-treatment temperature and fast quench rate in a large grain size material produces the ideal combination of heat-treatment and microstructural parameters for maximum non-equilibrium segregation. The influence of the vacancy impurity binding energy, E_b, on non-equilibrium segregation is nothing like so marked as either of the above-mentioned factors. As can be seen from Fig. 2, the segregation effect is large and reasonably constant over the range of E_b between 0.3 and 0.6 eV. This range is the range most commonly met in practice.

5. Conclusions

A model which estimates the magnitude and extent of non-equilibrium segregation to grain boundaries as a function of heat-treatment conditions has been described. The results predicted by the model show reasonable agreement with experimental measurements for three different segregating impurities in austenitic alloy matrices.

The model predicts that non-equilibrium segregation will occur if the vacancy–impurity binding energy is greater than 0.2 eV. If this is so then the following heat-treatment and microstructural parameters are likely to lead to maximum non-equilibrium segregation:

(a) high solution-treatment temperature;

(b) fast cooling from the solution-treatment temperature so that the critical time after which de-segregation begins to dominate, t_c, is not exceeded;

(c) no ageing treatment after the quench;

(d) large grain size.

Acknowledgements

Thanks are due to Dr A. M. Stoneham of UK Atomic Energy Authority, Harwell and Dr E. D. Hondros of National Physical Laboratory for useful discussions. The provison of facilities for this work by Professor I. A. Menzies of Loughborough University of Technology is gratefully acknowledged.

Appendix 1 Calculation of critical time, t_c

The time at which transition from segregation to de-segregation occurs is influenced by (a) the relative diffusion rates of the vacancy complexes and the impurities and (b) the grain size. This critical time, t_c, can be estimated by equating the flux of complexes towards the grain boundaries to the impurity flux towards the grain centres. These two fluxes represent the processes of segregation and de-segregation, respectively. The resultant equation is given by

$$\frac{2D_I\Delta c_I}{d} = \frac{2D_v\Delta c_v}{d}, \qquad \text{(A1)}$$

where D_I is the impurity diffusion coefficient in the matrix, D_v is the diffusion coefficient for the complexes in the matrix, Δc_I is the fraction of the maximum permissible impurity concentration found on the grain boundaries after non-equilibrium segregation, Δc_v is the fraction of the maximum permissible complex concentration found at the grain centres after non-equilibrium segregation, d is the grain size.

Δc_I and Δc_v are time-dependent concentrations which decrease when the mean diffusion distance for each species reaches the mean grain radius. Thus:

$$\Delta c_I = \exp\left(\frac{-t}{\tau_I}\right) \qquad \text{(A2)}$$

and

$$\Delta c_v = \exp\left(\frac{-t}{\tau_v}\right), \qquad \text{(A3)}$$

where t is time. The time after which decreased concentrations are expected to occur is defined by τ in each case as follows.

$$\tau_I = \frac{d^2}{4\delta D_I} \qquad \text{(A4)}$$

and

$$\tau_v = \frac{d^2}{4\delta D_v}, \qquad \text{(A5)}$$

where δ is a numerical constant. Therefore, when

Equations A2–A5 are substituted into Equation A1, the time, t, indicated will be that at which the diffusion flux of impurities away from the grain boundaries just begins to dominate the flux of complexes towards the grain boundaries. This time is the critical time, t_c, and is given by

$$t_c = \frac{\delta d^2 \ln (D_v/D_I)}{4(D_v - D_I)}. \quad \text{(A6)}$$

Appendix 2 Quantification of de-segregation

This section describes the derivation of Equation 15. The thin-film solution to Fick's Second Law gives the impurity concentration caused by non-equilibrium segregation at a point, x, from the grain boundary, c_x, relative to the impurity concentration in the centre of the grains after non-equilibrium segregation, c_g;

$$c_x - c_g = \frac{\alpha}{2(\Pi D_I t_\theta)^{1/2}} \exp\left(\frac{-x^2}{4D_I t_\theta}\right), \quad \text{(A7)}$$

where t_θ is the time elapsed since the beginning of non-equilibrium segregation ($t_\theta > t_c$), D_I is the impurity diffusion coefficient in the matrix. α is a concentration per unit area term evaluated as follows. α is the amount of impurity deposited on the grain boundary during the segregation part of the non-equilibrium segregation process. This amounts to the accumulation of impurities by the segregation process according to Equation 12 for a period of time t_c. Thus, at $x = 0$ and after time t_c, $c_x = c_b$, where c_b is the maximum permissible impurity concentration on the grain boundary, given by Equation 7. Up to this time the accumulation of impurity has been controlled by the supply of complexes. Hence the diffusion coefficient rate controlling term is D_v, where D_v is the diffusion coefficient for complexes in the matrix. Therefore, from Equation A7,

$$c_b - c_g = \frac{\alpha}{2(\Pi D_v t_c)^{1/2}}. \quad \text{(A8)}$$

Therefore

$$\alpha = 2(c_b - c_g)(\Pi D_v t_c)^{1/2}. \quad \text{(A9)}$$

Therefore, substituting α into Equation A7 gives

$$\frac{c_x - c_g}{c_b - c_g} = \left(\frac{D_v t_c}{D_I t_\theta}\right)^{1/2} \exp\left(\frac{-x^2}{4D_I t_\theta}\right). \quad \text{(A10)}$$

To find the impurity concentration on the grain boundary at any time during the de-segregation process, c_{x0}, x is simply equated to 0 in Equation A10 and, remembering that $t_\theta > t_c$, then

$$\frac{c_{x0} - c_g}{c_b - c_g} = \left(\frac{D_v t_c}{D_I t_\theta}\right)^{1/2} \quad \text{(A11)}$$

References

1. M. P. SEAH and E. D. HONDROS, *Int. Met. Rev.* **222** (1977) 262.
2. E. D. HONDROS and D. MCLEAN, "Surface Phenomena of Metals" Vol. 28 (London Society of Chemical Industry, London, 1968) p. 39.
3. M. GUTTEMANN, *Metal Sci.* **10** (1976) 337.
4. D. MCLEAN, "Grain Boundaries in Metals" (Clarendon Press, Oxford, 1957) p. 131.
5. M. P. SEAH, *Acta. Met.* **25** (1977) 345.
6. K. T. AUST, S. J. ARMIJO, E. F. KOCH and J. A. WESTBROOK, *Trans. Amer. Soc. Met.* **60** (1967) 360.
7. T. R. ANTHONY, *Acta Met.* **17** (1969) 603.
8. K. T. AUST, R. E. HANNEMAN, P. NIESSEN and J. H. WESTBROOK, *ibid.* **16** (1968) 291.
9. T. M. WILLIAMS, A. M. STONEHAM and D. R. HARRIES, *Metal Sci.* **10** (1976) 14.
10. D. R. HARRIES and A. D. MARWICK, *Phil. Trans. Roy. Soc.* **A295** (1980) 197.
11. A. H. COTTRELL, "An Introduction to Metallurgy", (Edward Arnold, London, 1967) p. 345.
12. B. L. EYRE and D. M. MAHER, AERE Report R-6618, UKAEA, Harwell, UK, December, 1970.
13. R. G. FAULKNER, T. C. HOPKINS and K. NORRGÅRD, *X-ray Spectrometry* **6** (1977) 73.
14. R. G. FAULKNER and B. J. E. ROSBORG, Studsvik Energiteknik, Sweden, unpublished work, 1978.
15. R. G. FAULKNER and K. NORRGÅRD, *X-ray Spectrometry* **7** (1978) 184.
16. R. G. FAULKNER and J. CAISLEY, *Metal Sci.* **11** (1977) 200.
17. M. E. WARGA and C. WELLS, *J. Metals* **5** (1953) 1463.
18. S. H. MOLL and R. E. OGILVIE, *Trans. Met. Soc. AIME* **215** (1959) 613.
19. R. A. SWALIN and A. MARTIN, *Met. Trans. AIME* **206** (1956) 567.
20. F. S. BUFFINGTON, K. HIRANO, M. COHEN, *Acta Met.* **9** (1961) 434.
21. J. R. MacEWAN, J. U. MacEWAN and L. YAFFE, *Canadian J. Chem.* **37** (1959) 1623.

Received 17 April and accepted 8 July 1980.